

Background contributions in gamma spectrometry

γ -SPEKT/NULLEF

Authors:

D. Arnold ¹

A. Heckel ²

H. Wershofen ¹

¹ Physikalisch-Technische Bundesanstalt
(Physikalisch-Technische Bundesanstalt – PTB)

² Federal Office for Radiation Protection
(Bundesamt für Strahlenschutz – BfS)

Background contributions in gamma spectrometry

1 Introduction

The background of an activity determination is that contribution to the pulse height spectrum which does not originate in the activity of the radionuclides contained in the counting source. The background consists of an intrinsic contribution of the gamma spectrometric measurement system and its surrounding as well as of contributions arising from the counting source consisting of the measurement container and of the substance to be measured.

To determine the activity of radioactive substances, it is indispensable to assess the net count rates of gamma peaks in the background spectrum. These gamma peaks must be taken into account when evaluating the pulse height spectrum of the sample. Furthermore, both the net count rates of background peaks and the background spectrum continuum influence the achievable detection limit when determining activity. As a rule, the measurement of the pulse height spectra of the background should be performed over a time at least as long as that taken to measure the pulse height spectra of the sample. In addition, they should be repeated at adequate intervals. More information on this topic can be found in the General Chapter γ -SPEKT/GRUNDL of this Procedures Manual.

For more details on the peaks occurring in the background pulse height spectrum and on the dependence of the background spectra on the type of detector or spectrometer are described in the following. Possible interferences of background contributions with gamma peaks of radionuclides to be determined are dealt with in the General Chapter γ -SPEKT/INTERF of this Procedures Manual.

Note:

All nuclear data used in this General Chapter is as of June 2018. Up-to-date values can be found in the General Chapter KERNDATEN of this Procedures Manual.

2 Origin of the background contributions

Background contributions can be divided into four groups, according to their origin:

— Radon progenies (group 1):

These peaks occur in particular when a larger amount of air is present within the detector shielding. Their intensity varies depending on the radon concentration present in the air of the laboratory. The air remaining in the inner part of the shielding therefore contributes to the spectrum continuum (Pb-214, Bi-214 as radon progenies) if it is not expelled, e. g., by purging with the nitrogen escaping from the dewar.

- Radionuclides contained in the components of the detector and of its shielding (group 2):
Among these are the primordial radionuclides K-40, U-238, U-235 and Th-232 with their short-lived progenies as well as Ra-226, Pb-210 with progenies, but also Co-60, which might occur in the form of impurities in construction materials.
- Activation products (group 3):
Neutrons from cosmic radiation generate short-lived radionuclides in the detector itself, its components and its shielding. Among these short-lived radionuclides are: Ge-71m, Ge-73m, Ge-75m, Cu-63, Cu-64, Cu-65.
- Inelastic neutron scattering (group 4):
Moreover, due to (n,n' γ) reactions in germanium, sawtooth-like broadened peaks may occur when the variable recoil energy and the energy of the gamma transition add up.

The background should be measured repeatedly to be able to reliably measure the specific activity and the activity concentration, respectively, of natural radionuclides in environmental samples, especially at low activity contents. The spectrum continuum of the measurement arrangements must therefore be kept as low and, in particular, as stable as possible by means of suitable measures (e. g. by keeping the shielding free of dust using lint-free wipes humidified with distilled water). Forced ventilation of the laboratory may contribute to stabilizing the background contributions of radon progenies. In this case, attention must be paid to the fact that the air drawn in from the outside may contain large quantities of radon due to the warming up of the soil (especially in spring when the soil is thawing). A more in-depth consideration of the subject and information on further possibilities of reducing background contributions in pulse height spectra, e. g., when operating gamma spectrometry measurement systems in underground laboratories, are given in the references [1] to [17].

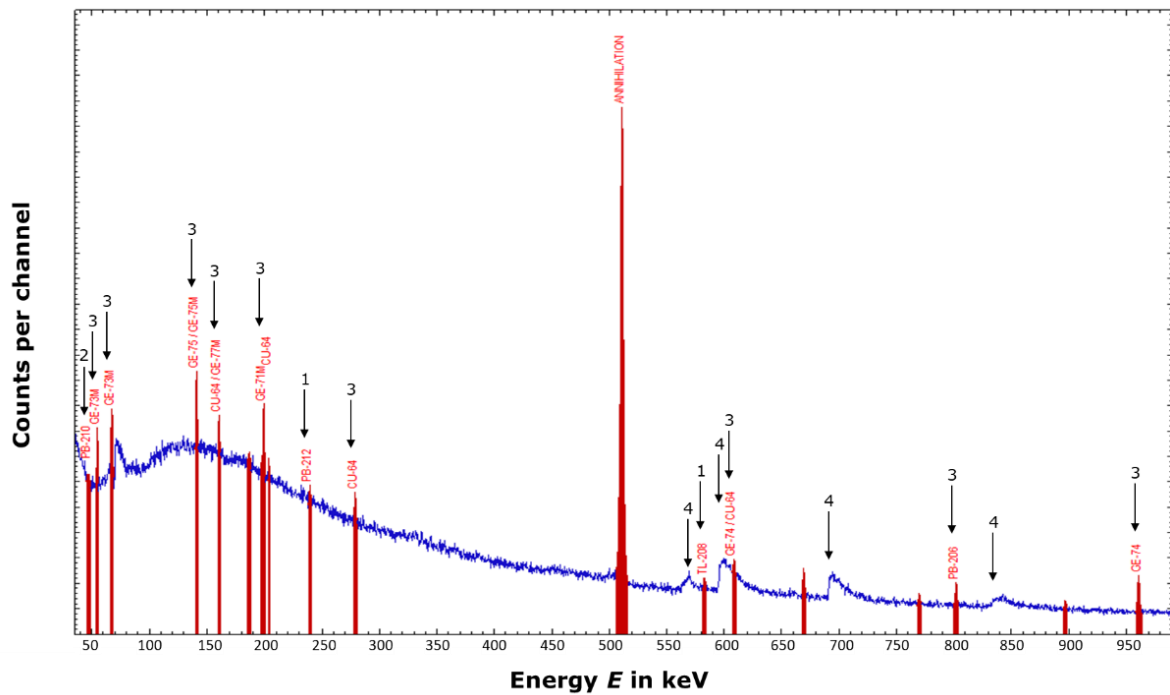


Fig. 1: Section of a pulse height spectrum providing examples for the four groups of peaks, with the peaks of group 3 and group 4 dominating, whereas peaks of group 4 are hardly identifiable. (Measurement with detector no. 6, without measurement container; duration of the measurement: $3,25 \cdot 10^5$ s).

Figure 1 shows typical background contributions in the energy region between 35 keV and approx. 970 keV. The pulse height spectrum was recorded with the low-level gamma spectrometric measurement system described in Table 1 as "Detector no. 6".

Tab. 1: Measurement arrangements used for measuring the pulse height spectra shown in the figures

Detector number	Detector specification	Particularity
3	<ul style="list-style-type: none"> – HPGe borehole-type detector – sensitive volume: 190 cm³ – relative detection efficiency (ϵ_{rel}): 41 % – Aluminium end cap 	<ul style="list-style-type: none"> – 20 cm thick, low-Pb-210 lead shielding with inner shielding made of 0,5 cm thick electrolytic copper – Purging with gaseous nitrogen – Operated in a basement room
5	<ul style="list-style-type: none"> – HPGe detector – sensitive volume: 50 cm³ – Aluminium end cap with beryllium window 	<ul style="list-style-type: none"> – reversed electrode – 10 cm thick, low-Pb-210 lead shielding with inner shielding made of 10 mm thick electrolytic copper as X-ray photon absorber – Operated in walk-in measuring chamber made of 10 cm thick, low-Pb-210 lead
6	<ul style="list-style-type: none"> – HPGe detector – sensitive volume: 202 cm³ – relative detection efficiency (ϵ_{rel}): 50 % – Aluminium end cap 	<ul style="list-style-type: none"> – 20 cm thick, low-Pb-210 lead shielding with inner shielding made of 0,5 cm thick electrolytic copper – Purging with gaseous nitrogen
7	<ul style="list-style-type: none"> – semi-planar HPGe detector – sensitive volume: 30 cm³ (surface: 2000 mm²; thickness: 15 mm) – End cap of electrolytic copper with low-uranium beryllium window 	<ul style="list-style-type: none"> – particularly sensitive in the energy region from 10 keV to 100 keV – 10 cm thick, low-Pb-210 lead shielding with inner shielding made of 10 mm thick electrolytic copper as X-ray photon absorber – Operated in walk-in measuring chamber made of 10 cm thick, low-Pb-210 lead
10	<ul style="list-style-type: none"> – Coaxial HPGe detector – sensitive volume: 311 cm³ – relative detection efficiency (ϵ_{rel}): 82 % – Aluminium end cap 	<ul style="list-style-type: none"> – 20 cm thick, low-Pb-210 lead shielding with inner shielding made of 0,5 cm thick electrolytic copper – Purging with gaseous nitrogen

Note:

The set-up of a standard shielding is described in [1].

3 Contribution of the detector background

The detector background usually designates the contributions from the measurement system and the environment.

The components located close to the detector should consist of materials that are, as far as possible, free of radioactive impurities. While systematically searching for materials with a low activity due to natural radionuclides in order to build the components of the detector, the historical pulse height spectra shown in Figure 2 were recorded.

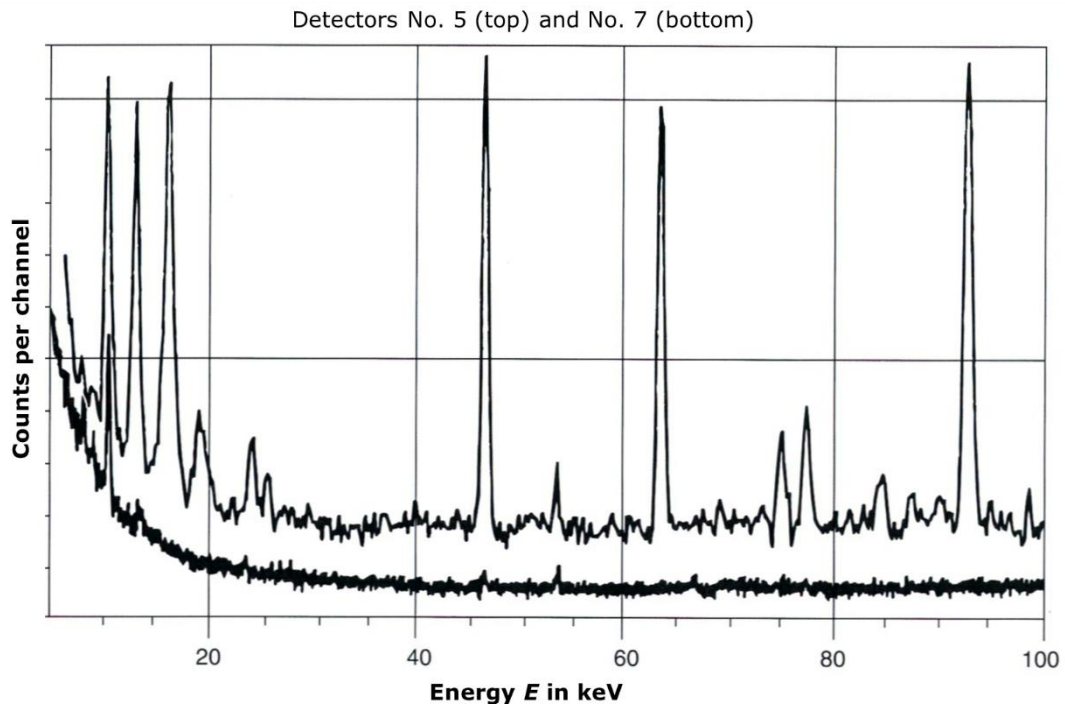


Fig. 2: Pulse height spectra of the detector background in the energy region below 100 keV, measured with two different detectors (detector no. 5 and detector no. 7) with a nearly identical shielding construction.

The differences in the two spectra result from the different detector materials. In the energy region from 40 keV to 100 keV, the influence of impurities caused by natural radionuclides in the end cap of detector no. 5 prevails. The gamma peaks below 40 keV are mainly due to activation products (group 3). Contrary to this, due to the materials composing the end cap of detector no. 7, it is mainly the X-ray peak at the energy of 10,4 keV which is detected. This X-ray peak arises as the summation peak of all X-ray K-, L- and M-fluorescence photons of stable gallium-71.

The effect of a lead shielding on the detector background is illustrated in Figure 3.

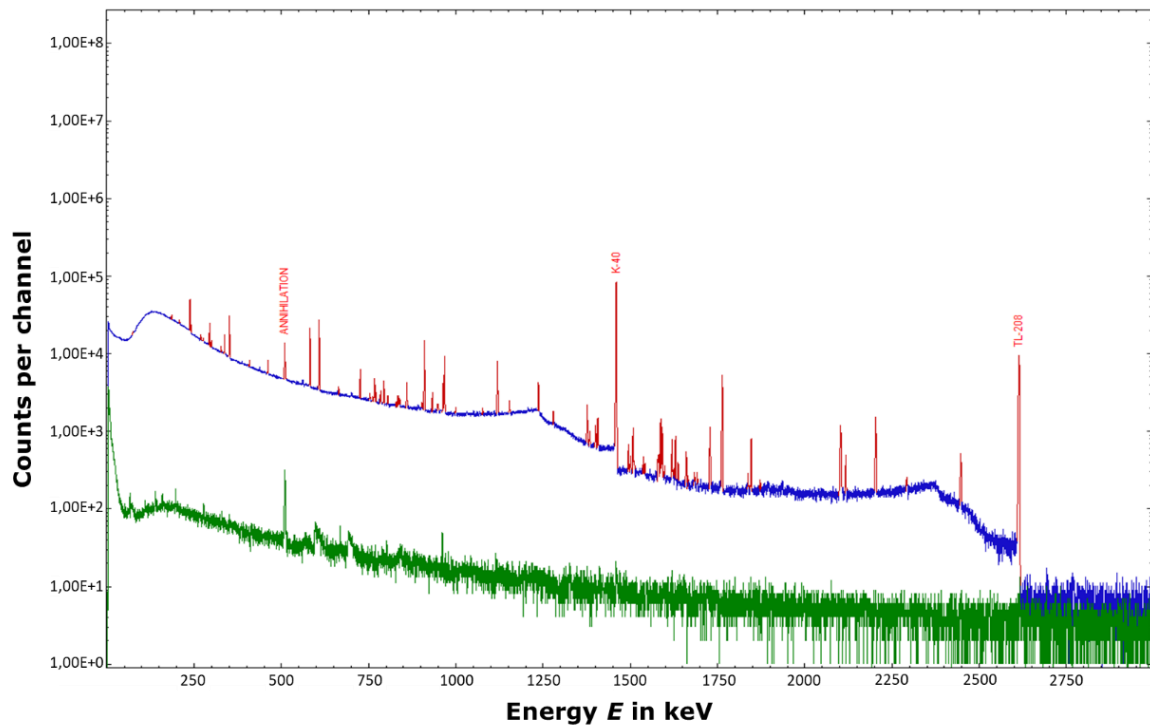


Fig. 3: Pulse height spectra of the detector background (detector no. 3) in the energy region from approx. 5 keV to approx. 3000 keV, measured without shielding (blue) and with a shielding in accordance with Table 1 (green) at practically the same duration of measurement. The representation of these spectra is normalized according to the duration of measurement.

In the pulse height spectrum without shielding, 77 peaks are clearly recognizable, whereas only 26 peaks are left in the pulse height spectrum with a shielding. A selection of these peaks is compiled in Table 2. The intensities of the peaks are clearly weaker with the shielding; peaks of group 4 only become visible at all due to the shielding.

Tab. 2: Compared count rates of selected background peaks, measured with detector no. 3 (see Table 1)
 (a) with shielding
 (b) without shielding

Energy of the peak in keV	Radionuclide	Count rate in s ⁻¹	
		(a)	(b)
186,03*	Cu-65, Ra-226, U-235	1,02E+00	2,49E-03
197,89	Ge-71m	n. d.	6,77E-03
209,16	Ac-228	6,63E-01	–
238,63	Pb-212	1,31E+00	–
242,00	Pb-214	7,53E-01	–
270,25	Ac-228	6,33E-01	–
295,22	Pb-214	8,52E-01	–
300,09	Pb-212	4,61E-01	–
328,00	Ac-228	3,96E-01	–
338,32	Ac-228	6,40E-01	–
351,93	Pb-214	8,43E-01	–
463,00	Ac-228	2,58E-01	–
511,00	Annihilation	6,72E-01	–
583,19	Tl-208	5,31E-01	–
609,26*	Ge-73, Bi-214	6,57E-01	1,75E-03
669,70	Cu-63	n. d.	1,38E-03
727,33	Bi-212	2,01E-01	–
768,36	Bi-214	1,99E-01	–
794,94	Ac-228	1,62E-01	–
860,53	Tl-208	1,60E-01	–
911,20	Ac-228	3,81E-01	–
934,06	Bi-214	1,15E-01	–
964,79	Ac-228	1,46E-01	–
962,68	Cu-63	n. d.	1,50E-03
968,96	Ac-228	2,46E-01	–
1115,48	Cu-65	n. d.	7,20E-04
1120,29	Bi-214	2,50E-01	–
1238,11	Bi-214	1,59E-01	–
1377,67	Bi-214	8,16E-02	–

Energy of the peak in keV	Radionuclide	Count rate in s ⁻¹	
		(a)	(b)
1407,98	Bi-214	6,77E-02	–
1417,70	Cu-63	n. d.	5,29E-04
1460,82	Ka-40	2,17E+00	5,26E-04
1509,23	Bi-214	3,76E-02	–
1588,20	Ac-228	1,20E-01	4,00E-04
1592,51	Th (Double Escape)**	4,12E-02	–
1729,60	Bi-214	3,94E-02	–
1764,49	Bi-214	1,55E-01	–
1847,42	Bi-214	2,87E-02	–
2103,51	Th (Single Escape**)	5,42E-02	–
2204,21	Bi-214	5,41E-02	–
2614,51	Tl-208	3,17E-01	4,86E-04

* Position of the peak consisting also of individual gamma peaks which cannot be resolved.

** see General Chapter γ -SPEKT/SUMESC of this Procedures Manual.

n. d. not detectable

Peaks induced by cosmic radiation can be further suppressed by operating the gamma spectrometric measurement system in a place such as an underground laboratory [4, 17]. This effect is illustrated in Figure 4. The four background spectra shown were recorded with detector no. 10 with and without shielding, in a counting room located in a basement and in an underground laboratory located in the former salt mine Asse II, respectively.

Note:

The underground laboratory was located at the 925 m level of the former salt mine Asse II. There, the gamma local dose rate only amounted to approx. 1 % of the local dose rate measured outdoors at the earth's surface. The intensity of the muon component of cosmic radiation was smaller by more than five orders of magnitude [17].

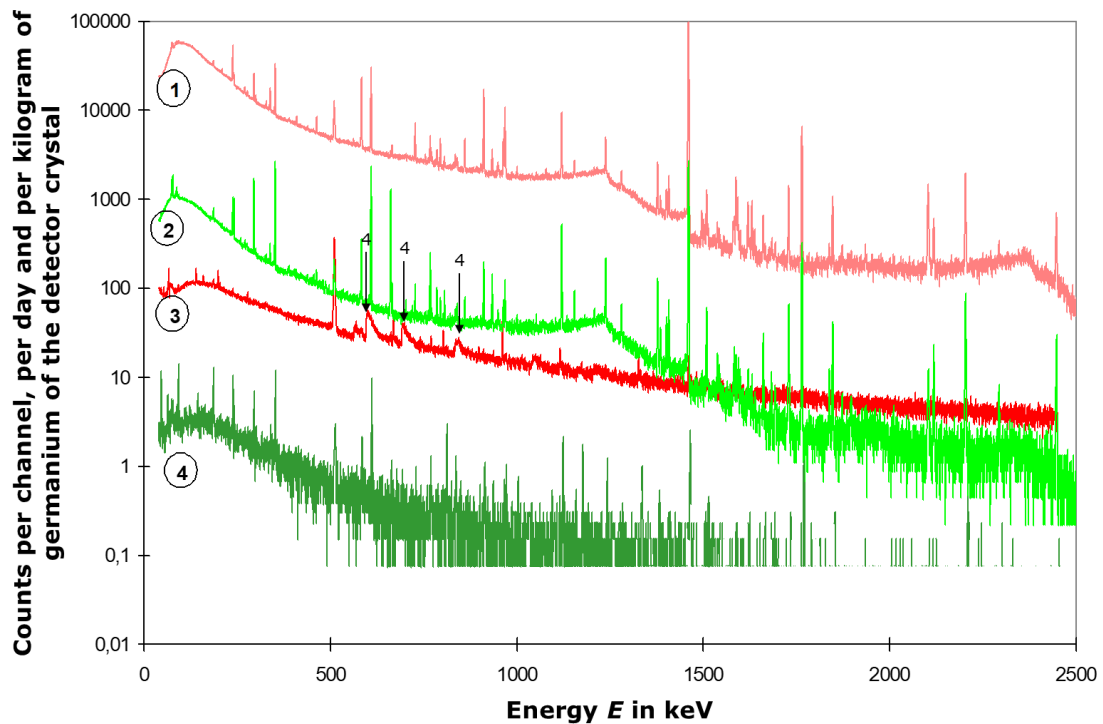


Fig. 4: Pulse height spectra recorded with detector no. 10.
1: without shielding; in a counting room located in a basement,
2: without shielding in the underground laboratory,
3: with shielding in a counting room located in a basement,
4: with shielding in the underground laboratory

The most obvious features in Figure 4 are the differences between the spectra 3 and 4: the group 4 background peaks, which are particularly prominent in spectrum 3, arise from an interaction between cosmic radiation and the germanium contained in the detector crystal and are no longer detectable in spectrum 4 due to the shielding effect of the overlying rock.

4 Contributions of the counting source

The counting source, consisting of the measurement container and the substance to be measured, also may contribute to the background pulse height spectrum.

To illustrate this contribution, two background measurements were carried out over particularly long durations of measurement with detector no. 6 as the gamma spectrometric measurement system; both measurements took place over a comparable duration of measurement of approx. $2,5 \cdot 10^6$ s:

- Measuring the contribution from the detector background (Det.-BG);
- Measuring the contribution from the detector background and the contribution from the counting source consisting of one litre of distilled water in a Marinelli beaker with a volume of one litre (H₂O-BG).

Figures 5 to 8 show the actually overlapping pulse height spectra. These are shifted for a better illustration of the individual effects. Therefore, they can only be compared qualitatively. Figures 6 to 8 show selected energy regions of the background spectra shown in Figure 5 to differentiate between peaks that lie close to each other more easily.

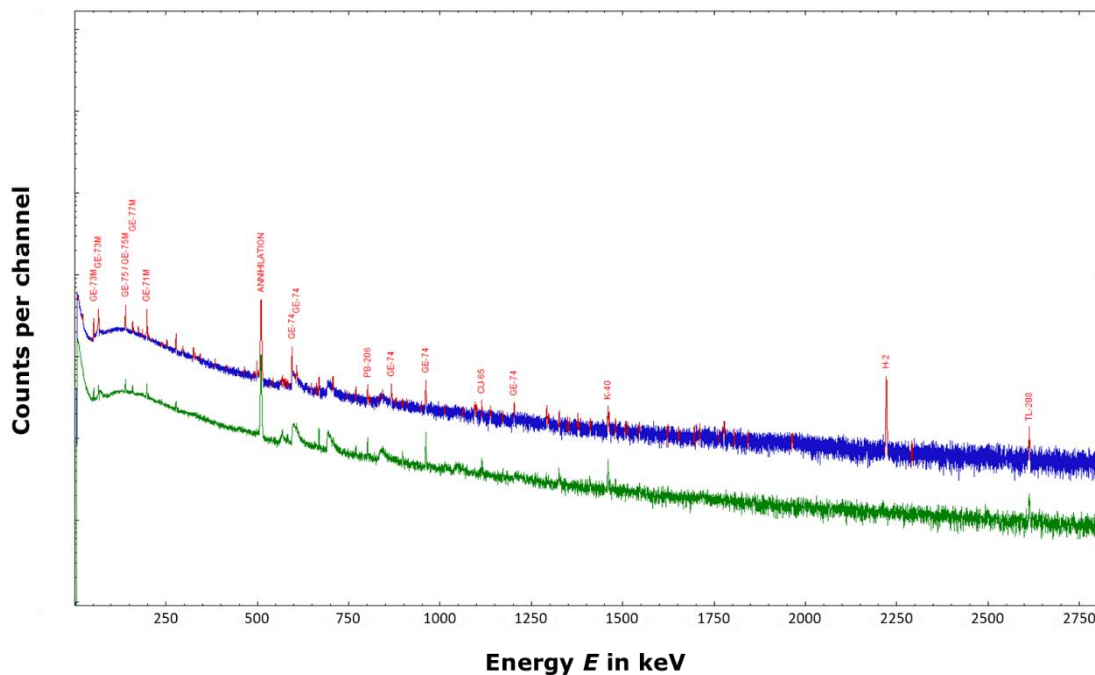


Fig. 5: Logarithmic representation of the background pulse height spectra Det.-BG (green) and H₂O-BG (blue).

The influence of one litre of distilled water on the pulse height spectrum of a background is illustrated in Figure 5:

- Water has a shielding effect.
- The water moderates neutrons from cosmic radiation.

As a consequence, the peaks generated by neutron interactions inside the germanium crystal itself and in the materials surrounding it are enhanced. These peaks are mostly peaks generated by prompt or delayed gamma photons after an n,γ or an $n,n'\gamma$ reaction. They are most of the time not included in common databases of nuclear data. Nuclear data concerning the assignment and interpretation of activation peaks and prompt gamma peaks are available online [12, 13].

At the same time, the H₂O-BG allows peaks to be detected that, in a pulse height spectrum imaging the detector background only, do not occur, are attenuated or enhanced.

Figure 6 illustrates the moderator effects of water in the energy region from 15 keV to 210 keV of a pulse height spectrum. This effect is particularly notable in the case of the Ge-71 gamma peak at 174,9 keV, which only occurs in the blue H₂O-BG spectrum.

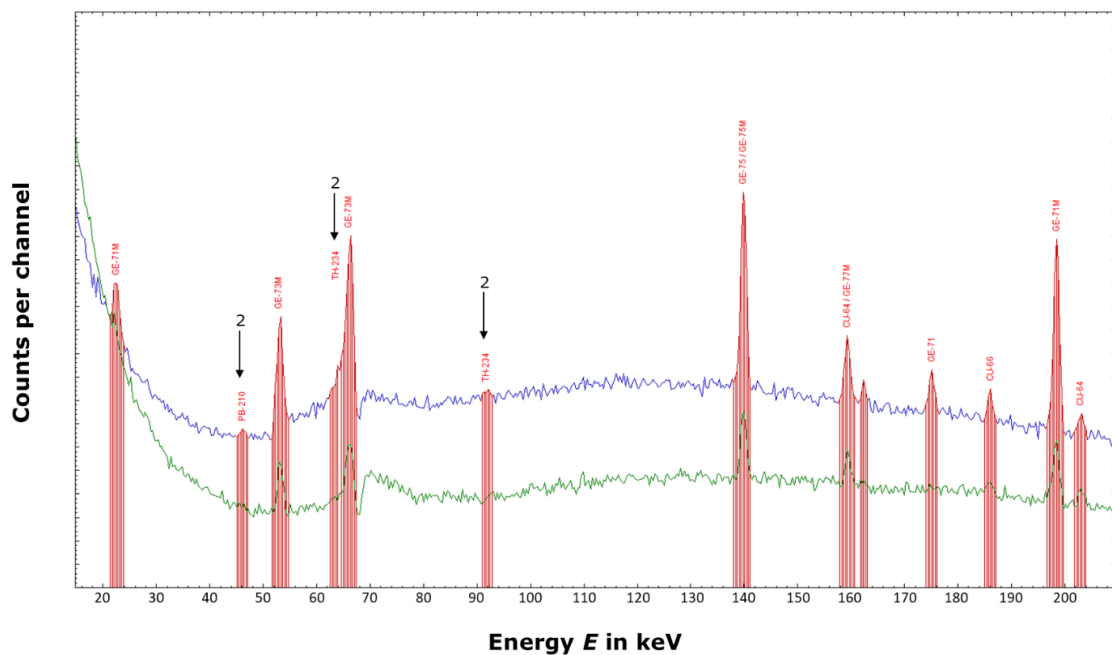


Fig. 6: Section of the energy region from 15 keV to 210 keV; the highlighted parts are the characteristic peaks that can be measured in addition to the other peaks or in an enhanced manner in the blue H₂O-BG spectrum.

In Figure 7, which shows the energy region from 450 keV to 820 keV, what is particularly notable – besides the annihilation peak at 511 keV – is the background peak at the energy of 595,8 keV, which is visible on the left edge of the sawtooth-like peak. This is the activation peak of Ge-74 from group 3 which is of cosmogenic nature.

Note:

In the case of high-sensitivity, low-level gamma spectrometric measurement systems, the gamma peak of Kr-85 may occur at 514,0 keV in background spectra with a long duration of measurement if technical-grade liquid nitrogen is used for cooling as it may contain traces of krypton [14, 15].

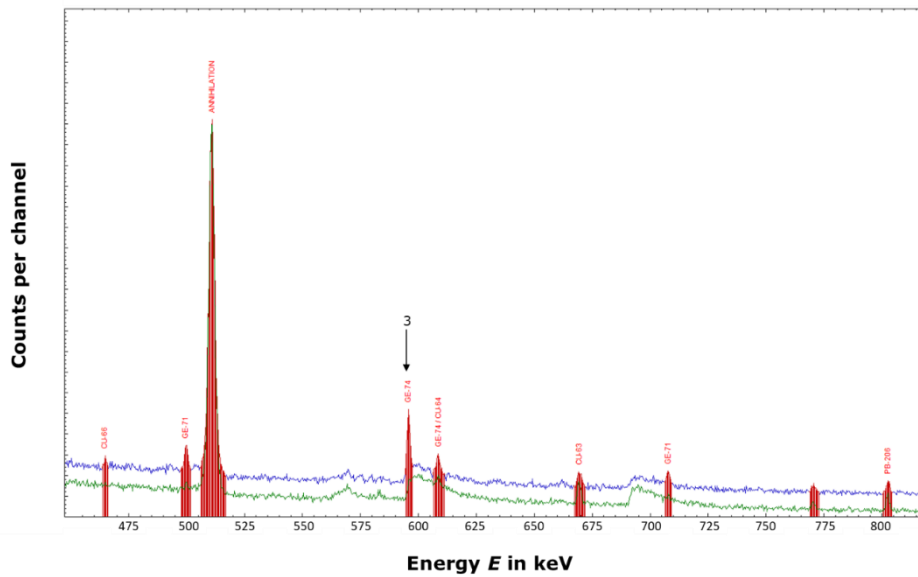


Fig. 7: Section of the energy region from 450 keV to 820 keV; the parts highlighted in red are the characteristic peaks that can be measured in addition to the other peaks or in an enhanced manner in the blue H₂O-BG spectrum.

Figure 8 shows the energy region from 1080 keV to 1480 keV. The following peaks are important in this section:

- the overlapping gamma peaks of Cu-65 at 1115,5 keV and of Zn-65 at 1115,7 keV, which are caused by cosmic radiation [16];
- the doublet of peaks due to the cosmogenic activation peak of Kr-84 at 1463,9 keV and the K-40 peak at 1460,8 keV.

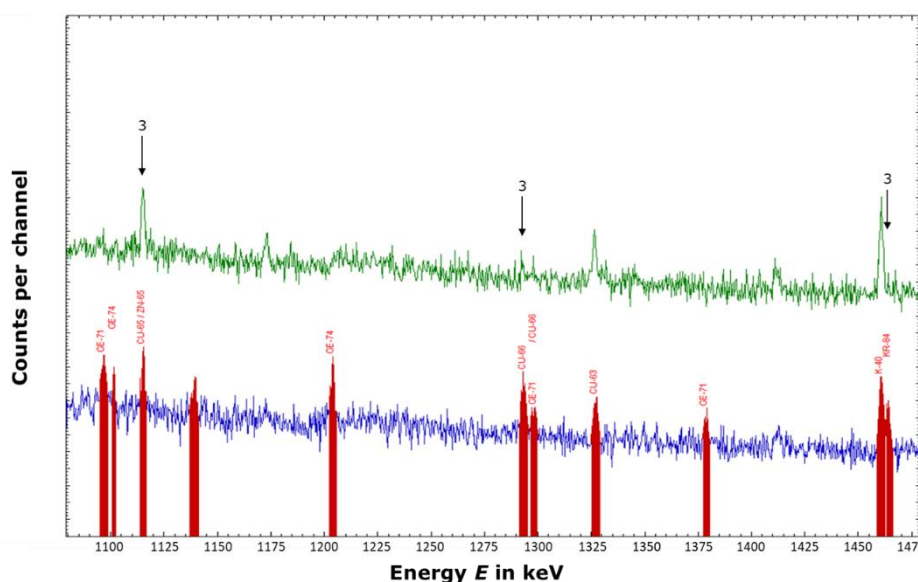


Fig. 8: Energy region from 1080 keV to 1480 keV; the parts highlighted in red are the characteristic peaks that can be measured in addition to the other peaks or in an enhanced manner in the blue H₂O-BG spectrum.

Table 3 lists a selection of the background peaks observed in the pulse height spectra shown in Figures 5 to 8 and their count rate ratio H₂O-BG/Det.-BG. In the case of weak peaks, the count rate ratios between approx. 0,8 and 1,2 are practically equivalent due to the relatively high statistical measurement uncertainty. There is, thus, no significant effect between Det.-BG and H₂O-BG.

Tab. 3: Selection of characteristic peaks in the background spectra H₂O-BG and Det.-BG from Figure 5 to illustrate the moderator effect of water

Peak with the energy	Count rate H ₂ O-BG	Count rate Det.-BG	Count rate ratio H ₂ O-BG/Det.-BG	Origin/radionuclide
in keV	in s ⁻¹	in s ⁻¹		
10,36	9,6E-04	1,8E-04	5,3	Ga- Σ K,L,M
22,80	9,0E-04	2,2E-04	4,1	In-116
53,47	1,9E-03	7,7E-04	2,5	Ge-73m
66,75	3,5E-03	1,1E-03	3,2	Ge-73m
139,20	3,2E-03	1,2E-03	1,0	Ge-75m
159,50	1,1E-03	4,5E-04	2,7	Ge-77m
174,88	6,8E-04	–		Ge-71
186,01	3,9E-04	2,1E-04	1,9	Cu-66
197,90	3,4E-03	1,3E-03	2,6	Ge-71m
202,95	3,4E-04	3,2E-04	1,1	Cu-64
278,24	1,3E-03	4,7E-04	2,8	Cu-64
298,66	2,1E-04	–		In-116
326,00	7,5E-04	–		Ge-71
343,94	2,5E-04	–		Cu-64
465,15	1,3E-04	–		Cu-66
492,94	8,2E-05	–		Ge-74
499,85	6,4E-04	7,0E-05	9,1	Ge-71
511,00	1,6E-02	1,7E-02	0,94	Annihilation
513,99	–*	*		Kr-85
595,85	3,2E-04	9,5E-05	3,4	Ge-74
608,35	5,1E-04	1,9E-04	2,7	Ge-74
669,60	5,2E-04	5,0E-04	1,1	Cu-63
803,00	3,7E-04	3,7E-04	1,0	Pb-206
867,90	3,6E-04	–		Ge-74
961,05	6,7E-04	–		Ge-74
962,68	–	7,6E-04		Cu-63
1063,60	7,7E-05	–		Pb
1101,27	7,7E-05	–		Ge-74

Peak with the energy	Count rate H ₂ O-BG	Count rate Det.-BG	Count rate ratio H ₂ O-BG/Det.-BG	Origin/radionuclide
in keV	in s ⁻¹	in s ⁻¹		
1115,48	1,5E-04	–		Cu-65
1115,54	1,5E-04	–		Zn-65
1139,65	9,7E-05	–		Cu-66
1204,21	1,8E-04	–		Ge-74
1293,59	2,2E-04	–		Sn-116
1298,80	7,8E-05	–		Ge-71
1327,00	2,0E-04	7,4E-05	2,6	Cu-63
1378,80	9,1E-05	–		Ge-71
1411,70	9,4E-05	2,3E-05	4,1	Cu-63
1463,86	1,8E-04*	–		Kr-84
1481,75	9,8E-05	6,5E-05	1,5	Cu-64
1777,80	1,4E-04	–		Ge-71
2223,30	1,7E-03 ⁺	–		H-2

* Technical-grade liquid nitrogen contains traces of krypton [14, 15].

⁺ In the background spectra of aqueous sources to be measured with large volumes, the gamma peak of H-2 at 2223,3 keV also appears. It is caused by the activation of natural hydrogen by cosmogenic neutrons.

References

- [1] DIN 25702:1995, *Abschirmungen von Detektoren für nuklidspezifische Aktivitätsmessungen*.
- [2] Debertain, K.: *Meßanleitung für die Bestimmung von Gammastrahlen-Emissionsraten mit Germanium-Detektoren*. PTB Ra-12, Braunschweig: PTB, September 1980.
- [3] Gehrke, R. J., Davidson, J. R.: *Aquisition of quality γ -ray spectra with HPGe spectrometers*. Appl. Radiat. Isot., 2005, Vol. 62, pp. 479–499. ISSN 0969-8043.
- [4] Laubenstein, M., Hult, M., Gasparro, J., Arnold, D., Neumaier, S., Heusser, G., Köhler, M., Povinec, P., Reyss, J.-L., Schwaiger, M., Theodorsson, P.: *Underground measurements of radioactivity*. Appl. Radiat. Isot., 2004, Vol. 61, pp. 167–172. ISSN 0969-8043.
- [5] Jovancevic, N., Krmar, M., Mrda, D., Slivka, J., Biki, I.: *Neutron induced background gamma activity in low-level Ge-spectroscopy systems*. Nucl. Instr. Meth. Phys. Res. A, 2010, Vol. 612, pp. 303–308.
- [6] Ljungvall, J., Nyberg, J.: *A study off ast neutron interactions in high-purity germanium detectors*. Nucl. Instr. Meth. Phys. Res. A, 2005, Vol. 546, pp. 553–573.

-
- [7] Roy, J.-C., Cöte, J.-E., Durham, R. W., Joshi, S. R.: *A study of the indium and germanium photo peaks in the background spectra of Ge spectrometers with a passive shield*. J. Radioanal. Nucl. Chem., 1989, Vol. 130, pp. 221–230. ISSN 0236-5731.
- [8] Mouchel, D.: *A high-purity-Ge detector system for the measurement of low-level radioactivity in environmental samples*. In: Garcia-Leon, M., Madurga, G., eds.: *Low-level measurements of manmade radionuclides in the environment*. Proceedings of the Second International School, Rabida, Huelva, Spain, 25 June to 6 July 1990. World Scientific Publishing Co., 1991, pp. 106–118.
- [9] Lindstrom, R. M., Lindstrom, D. J., Slaback, L. A., Langland, J. K.: *A low-background gamma-ray assay laboratory for activation analysis*. Nucl. Instr. Meth. Phys. Res. A, 1990, Vol. 229, pp. 425–429.
- [10] Heusser, G.: *Studies of gamma-ray background with a low-level germanium spectrometer*. Nucl. Instr. Meth. Phys. Res. B, 1991, Vol. 58, pp. 79–84.
- [11] Breier, R., Povinec, P.: *Simulation of background characteristics of low-level gamma-ray spectrometers using Monte Carlo method*. Appl. Radiat. Isot., 2010, Vol. 68, pp. 1231–1235. ISSN 0969-8043.
- [12] Brookhaven National Nuclear Data Center, Upton, NY, USA: *Thermal Neutron Capture Gammas by Energy (CapGam by Energy)*. Available at: <https://www.nndc.bnl.gov/capgam/indexbye.html>, [last accessed on 15 April 2019].
- [13] International Atomic Energy Agency (IAEA), Vienna, Austria: *Evaluated Gamma-ray Activation File (EGAF)*. Available at: <https://www-nds.iaea.org/pgaa/egaf.html>, [last accessed on 15 April 2019].
- [14] Zusel, G., Simgen, H., Heusser, G.: *Ar and Kr concentrations in nitrogen as a measure of the ³⁹Ar and ⁸⁵Kr activities in connection with the solar neutrino experiment Borexino*. Appl. Radiat. Isot., 2004, Vol. 61, pp. 197–201. ISSN 0969-8043.
- [15] Simgen, H., Heusser, G.: *Analysis of radioactive trace impurities with μBq-sensitivity in Borexino*. Internat. J. Mod. Phys. A, 2014, Vol. 29, No. 16.
DOI: 10.1142/S0217751X14420093.
- [16] Verplancke, J., Fettweis, P. F., Venkatarman, R., Young, B. M., Schwenn, H.: *Chapter 5: Semiconductor Detectors*. In: L'Annunziata, M. F., ed.: *Handbook of Radioactivity Analysis*. 3rd Edition. Amsterdam (the Netherlands): Elsevier Academic Press, 2012, pp. 320–326. ISBN 978-0-12-0384873-4.
- [17] Neumaier, S., Arnold, D., Böhm, J., Funck, E.: *The PTB underground laboratory for dosimetry and spectrometry*, Appl. Radiat. Isot., 2000, Vol. 53, pp. 173–178. ISSN 0969-8043.